Superlattice ordered structures of $(A_xA_{1-x})BO_3$ complex perovskite materials

1990 J. Phys.: Condens. Matter 2 9815

(http://iopscience.iop.org/0953-8984/2/49/008)

J. Phys.: Condens. Matter **2** (1990) 9815–9820. Printed in the UK

Superlattice ordered structures of $(A_xA_{1-x})BO_3$ complex perovskite materials

Qiang Wang†, Binglin Gu‡ and Xiaowen Zhang§

† Department of Materials Science and Engineering, Tsinghua University, Beijing 100084, People's Republic of China

‡ Department of Physics, Tsinghua University, Beijing 100084, People's Republic of China

§ Department of Materials Science and Engineering, Tsinghua University, Beijing 100084, People's Republic of China

Received 6 April 1990, in final form 14 July 1990

Abstract. Experimental observation of a $(Pb_{1-x}Ca_x)TiO_3$ complex perovskite ceramic near $x = 0.5$ has suggested that the Pb and Ca atoms are ordered alternately on a particular A site (111) plane. Furthermore, a body-centred superlattice ordered structure has been observed in $(Ba_{1-x}Pb_x)TiO_3$ ceramic. In this paper, the eight-point cluster variation method, in which the second- and third-neighbour interactions are considered, has been employed to study these ordered structures and calculate the phase diagrams as a function of reduced temperature and composition for various interaction parameters. Theoretical results explained well the formation mechanism of these ordered structures.

1. Introduction

Following the observation by Harmer, Cross and Setter and others [1, 2, 3] of B-site superlattice ordered structures in both $Pb(Sc, Ta)O_3$ (PST) and $Pb(Mg, Nb)O_3$ (PMN) perovskites, A-site superlattice ordered structures have also been observed in A-site complex perovskites [4, 5]. Systematically studying the $(Pb_{1-x}Ca_x)TiO_3$ complex perovskite with different values of x, Grace *et al* [4] found three kinds of superlattice reflections: $G \pm \frac{1}{2}\langle 111\rangle^*$, $G \pm \frac{1}{2}\langle 110\rangle^*$ and $G \pm \frac{1}{2}\langle 001\rangle^*$ near $x = 0.5$. Three possible Pb/Ca ordering patterns—which we label $\frac{1}{2}\langle 111\rangle$, $\frac{1}{2}\langle 110\rangle$ and $\frac{1}{2}\langle 001\rangle$ respectively (see figure 1)—were considered to be compatible with the unit cell of the superstructure they deduced. Only the former, however, was compatible with their dark field imaging results. King *et al* considered that the alternative arrangement of the Pb's and Ca's on (111) planes would give rise to $G \pm \frac{1}{2}\langle 111\rangle^*$ satellite reflections corresponding to the $\frac{1}{2}\langle 111\rangle$ ordered structure. At the same time, they proposed that additional atomic shifts or shuffles resulted in the latter two kinds of reflections in order to be consistent with experiment. However, Randall *et al* [5, 6] considered the formation of ordered structure to be due to the complex coupling between A-site and B-site sublattices. Moreover, they observed the body-centred superlattice in $(Ba_{1-x}Pb_x)TiO_3$ perovskite, and found that the reflection intensity increases as the composition of Ba ions decreases, and the Pb cations and Pb vacancies formed a complete ordered body-centred superlattice at $x = 1$ as shown in

0953-8984/90/499815 + 06 $03.50

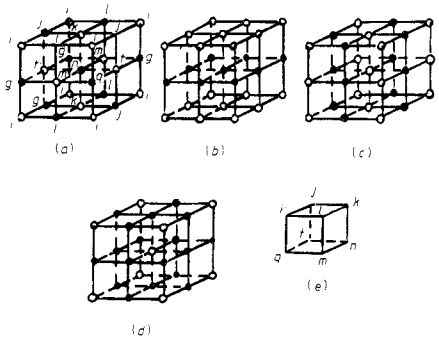

Figure 1. Some types of ordered structures. (*a*) $\frac{1}{2}\langle 111\rangle$; (*b*) $\frac{1}{2}\langle 100\rangle$; (*c*) $\frac{1}{2}\langle 110\rangle$; (*d*) $\frac{1}{4}$-type edge-centred; (*e*) selection of eight-point clusters.

figure 1(*d*). However, neither Randall *et al* nor King *et al* explained the formation mechanism of these ordered structures in perovskites satisfactorily.

The authors have studied the formation of B-site ordered structures and present a mechanism in [7]. However this model is unsuitable for A-site complex perovskite. In this paper, based on the eight-point cluster variation method including the second and third interactions, phase diagrams are calculated for various interaction parameters. Theoretical results are in agreement with experimental measurements.

2. Method

The crystal structure of ABO_3-type perovskite is simple cubic. Let us focus our attention on the A-site sublattice by introducing coupling between A-site, B-site and O-site sublattices into the interaction parameters. In $(Pb_{1-x}Ca_x)TiO_3$, $(Ba_{1-x}Pb_x)TiO_3$ and $(V(Pb)_{1-x}Pb_x)TiO_3$, etc the arrangements of A-site cations differ with composition x (shown in figure 1). In order to describe various A-site ordered structures in a unified framework, the A-site simple cubic lattice with $a = a_0$ is divided into eight equivalent interpenetrating simple cubic superlattices with $a = 2a_0$, where near-neighbour points constitute the eight-point cluster '*ijklmntq*' shown in figure 1(*e*). The arrangements of A-site cations depend on the distributions of A cations on the cluster.

$W_{ijklmntq}$ are defined as cluster occupation probabilities, where i, j, k, l, m, n, t, q can be taken as 1 or -1, referring to the point occupied by A or A cations, S_{ijkl}, S_{ijtq}, S_{jknt}, S_{klmn}, S_{ilmq} and S_{mntq} are four-point subcluster occupation probabilities; $X_{ij}, X_{il}, X_{iq}, \ldots,$ X_{tq} are pair occupation probabilities; $P_i, P_j, P_k, P_l, P_m, P_n, P_t, P_q$ are point occupation probabilities. They satisfy the following self-consistent relations:

$$1 = \sum_i P_i \qquad P_i = \sum_j X_{ij} \qquad X_{ij} = \sum_{kl} S_{ijkl}$$
$$S_{ijkl} = \sum_{mntq} W_{ijklmntq} \qquad P(i=1) + P(j=1) + \ldots + P(q=1) = 8x \tag{1}$$

where x is the composition of A-site cations.

According to the quasi-chemical method given by Sanchez [8], the configuration number can be written in terms of probability as follows:

$$\Omega = PS^3/x^3W. \tag{2}$$

The entropy is given by

$$S = K_B \ln \Omega \tag{3}$$

where K_B is the Boltzmann constant.

The average energies of the cluster are

$$\begin{aligned} E_{ijklmntq} = {} & \tfrac{1}{4}J_1(\sigma_i\sigma_j + \sigma_i\sigma_l + \sigma_i\sigma_q + \sigma_j\sigma_k + \sigma_j\sigma_t + \sigma_k\sigma_l + \sigma_k\sigma_n \\ & + \sigma_l\sigma_m + \sigma_m\sigma_n + \sigma_m\sigma_q + \sigma_n\sigma_t + \sigma_t\sigma_q) \\ & + \tfrac{1}{4}J_2(\sigma_i\sigma_k + \sigma_i\sigma_m + \sigma_i\sigma_t + \sigma_j\sigma_l + \sigma_j\sigma_n + \sigma_j\sigma_q + \sigma_k\sigma_m \\ & + \sigma_k\sigma_t + \sigma_l\sigma_n + \sigma_l\sigma_q + \sigma_m\sigma_t + \sigma_n\sigma_q) \\ & + \tfrac{1}{4}J_3(\sigma_i\sigma_n + \sigma_j\sigma_m + \sigma_k\sigma_q + \sigma_l\sigma_t) \end{aligned} \tag{4}$$

where J_1, J_2 and J_3 are respectively the nearest and second- and third-nearest-neighbour interactions between A-site cations; i refers to the site of the ith sublattice and can be taken as 1 or -1, corresponding to A or A cations. $\sigma_1 = 1$ and $\sigma_{-1} = -1$; the $E_{ijklmntq}$ have 14 non-equivalent values for different distributions of A cations.

The extended free energy of the system is

$$F = E - TS + \mu Nx = N \sum_{ijklmntq} W_{ijklmntq} E_{ijklmntq} - NK_B TS + \mu Nx. \tag{5}$$

Substituting equations (1) and (3) into (5) and minimizing the free energy with $W_{ijklmntq}$, the following iterative equation can be obtained:

$$\begin{aligned} W_{ijklmntq} = {} & [\exp(-E_{ijklmntq}/K_B T) \exp(-\mu a_{ijklmntq}/8K_B T) \\ & \times (P_i P_j P_k P_l P_m P_n P_t P_q)^{1/8} (X_{ij} X_{il} X_{iq} X_{jk} X_{jt} X_{kn} X_{kl} X_{lm} X_{mn} \\ & \times X_{nt} X_{tq} X_{mq})^{-1/4} (S_{ijkl} S_{ijtq} S_{jtkn} S_{kjmn} S_{ijmq} S_{mntq})^{1/2}] \\ & \times \left(\sum_{ijklmntq} W_{ijklmntq} \right)^{-1} \end{aligned} \tag{6}$$

where $\mu = \mu_{A_2} - \mu_{A_1}$ is the chemical potential and the $a_{ijklmntq}$ can take values from 1.0 to 8.0.

Using equations (1), (2) and (6) the iteration calculation was performed and the distributions of A-site cations on the cluster were obtained.

3. Results

From an analysis of the 14 types of cluster energies, the phase diagrams in (x) interaction parameter space were obtained for various compositions at $T = 0$ as shown in figure 2. Figure 2(a) shows that $\frac{1}{2}\langle 111\rangle$, $\frac{1}{2}\langle 110\rangle$ and $\frac{1}{2}\langle 100\rangle$-type ordered structures can occur at $x = 0.5$. Formation of the latter two ordered structures depends on the second and third interactions. Figure 2(c) shows that when $x = 0.25$ there are probably three kinds of ordered structures: body-, edge- and bottom-centred superlattices. When the second

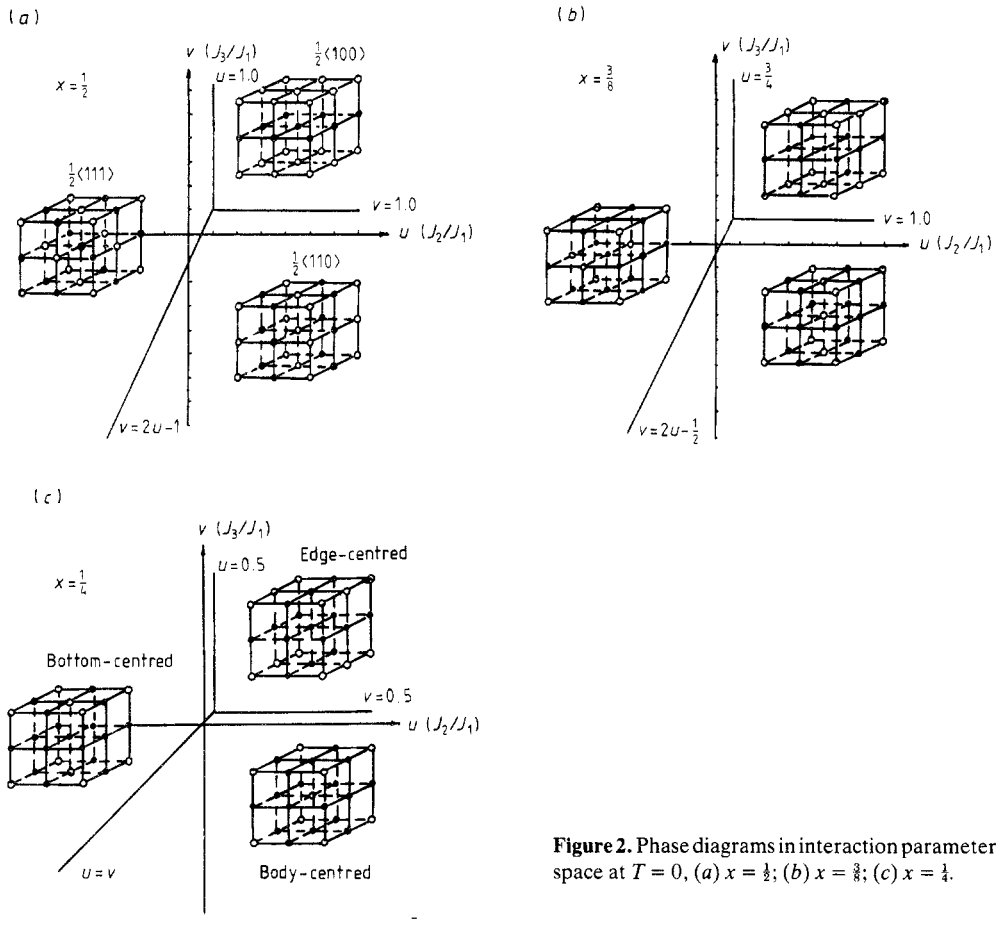

Figure 2. Phase diagrams in interaction parameter space at $T = 0$, (*a*) $x = \frac{1}{2}$; (*b*) $x = \frac{3}{8}$; (*c*) $x = \frac{1}{4}$.

interaction is the inverse of the third interaction, the body-centred superlattice ordered structure is stable. However, the free energy will vary with increasing temperature because of the configurational entropy. Phase diagrams as a function of reduced temperature and composition were obtained using equation (7). Let us now consider the following situations.

(i) $u = 0$, $v = 0$, i.e. only near-neighbour interaction is considered. There is not only the $\frac{1}{2}\langle 111\rangle$-type ordered structure at about $x = 0.5$, but also a $\frac{1}{4}$-type ordered structure near $x = \frac{1}{4}$. Because both the $\frac{1}{4}$-type bottom-centred and body-centred ordered structures probably occur simultaneously in this region of interaction parameter and composition, it is difficult to determine the structure of the system as shown in figure 3(*a*).

(ii) $u = -1.0$, $v = 0$. The system tends to be the $\frac{1}{2}\langle 111\rangle$ ordered state at about $x = 0.5$ and bottom-centred ordered structure at about $x = \frac{1}{4}$. The calculated phase diagram shows a widening of these order ranges at low temperature, as shown in figure 3(*b*).

(iii) $u = 1.0$, $v = 0$. The phase diagram (figure 3(*c*)) shows that the $\frac{1}{2}\langle 110\rangle$-type ordered structure exists in a narrow region of composition near $x = 0.5$ and a $\frac{1}{4}$-type body-centred structure also occurs in a narrow region of composition near $x = 0.25$.

(iv) $u = 1.5$, $v = 1.5$. Figure 3(*d*) shows that the $\frac{1}{2}\langle 100\rangle$ ordered structure appears in the composition region from $x = 0.5$ and also that the edge-centred structure can be stable at high temperature.

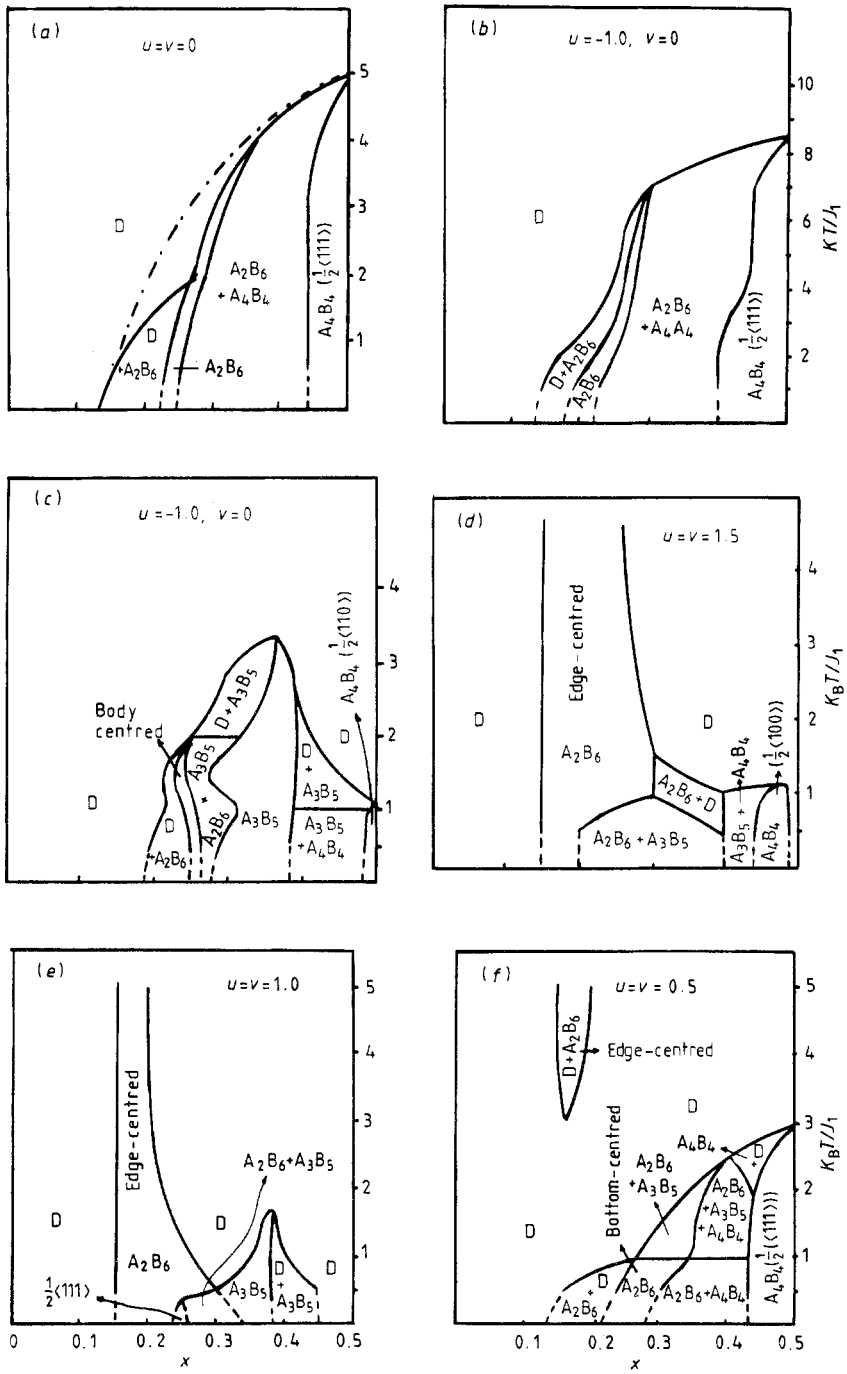

Figure 3. Phase diagrams as a function of reduced temperature (KT/J_1) and composition (x). (*a*) $u = 0$, $v = 0$. The broken curve shows the low-temperature extrapolation; the chain curve corresponds to the results of the pair-probability model; D, disordered state; A_2B_6, $\frac{1}{3}$-type ordered state; A_4B_4, $\frac{1}{2}$-type state. (*b*) $u = -1.0$, $v = 0$. A_2B_6, $\frac{1}{4}$-type body-centred superlattice whose ordering region is widened. (*c*) $u = 1.0$, $v = 0$. A_3B_5, $\frac{3}{8}$-type ordered state. (*d*) $u = v = 1.5$. (*e*) $u = v = 1.0$. (*f*) $u = v = 0.5$.

(v) $u = v = 1.0$. The three $\frac{1}{2}$-type ordered structures have the same ground energies. The phase diagram indicates that the $\frac{1}{2}$-type order does not occur at the whole range of temperature when $x = 0.5$. But the $\frac{1}{2}$-type partial ordered structure appears near $x = 0.25$ at low temperature, as shown in figure 3(*e*).

(vi) $u = v = 0.5$. The three $\frac{1}{4}$-type ordered structures have the same ground energies. The calculated results show that only the bottom-centred structure appears in the normal temperature range, the edge-centred structure occurs at relatively high temperature, and the body-centred structure never exists in this region of interaction parameters as shown in figure 3(*f*).

4. Discussion

The results calculated above show that the second and third interactions are necessary for the appearance of the $\frac{1}{2}\langle 110\rangle$, $\frac{1}{2}\langle 100\rangle$ and $\frac{1}{4}$-type body-centred structures. The second and third interactions are related to many factors, such as the electrostatic and elastic energies as well as cohesion. These ordered structures, however, are not stable at relatively high temperature. Interestingly, for the $(Ba_{1-x}Pb_x)TiO_3$ system the composition ratio within the $\frac{1}{4}$-type ordered domain is V(Pb) : Pb = 1 : 3, but not Ba : Pb = 1 : 3. This is probably due to the occupation of vacancies causing the formation condition for the ordered structure to be easily satisfied, i.e., the occupation decreases the energy of the ordered system. In the $(V(Pb)_{1-x}Pb_x)TiO_3$ system x stands for the stoichiometry of A-site vacancies but not oxygen vacancies. Therefore the CVM approach based on the A sites remains valid.

References

[1] Harmer M P, Bhalla A and Cross L E *et al* 1984 *Mater. Lett.* **2** 278
[2] Setter N and Cross L E 1980 *J. Appl. Phys.* **51** 4356; 1980 *J. Mater. Sci.* **15** 2478
[3] Chen J, Chan H M and Harmer M P 1989 *J. Am. Ceram. Soc.* **72** 593
[4] Grace K *et al* 1988 *J. Am. Ceram. Soc.* **71** 454
[5] Randall C *et al* 1987 *Ferroelectrics* **76** 277
[6] Randall C *et al* 1989 *Phys. Rev.* B **40** 413
[7] Wang Qiang, Gu Binglin and Zhang Xiaowen 1989 *Acta Phys. Sin.* **38**
[8] Sanchez J M *et al* 1978 *Phys. Rev.* B **17** 2926